Superconducting Cuprates and Related Oxides. I. Solid State Preparation and X-Ray Characterization of Selected Binary, Ternary and Quaternary Oxides

A. Nørlund Christensen

Department of Inorganic Chemistry, Aarhus University, DK-8000 Aarhus C, Denmark

Christensen, A. N., 1990. Superconducting Cuprates and Related Oxides. I. Solid State Preparation and X-Ray Characterization of Selected Binary, Ternary and Quaternary Oxides. – Acta Chem. Scand. 44: 769–776.

Solid state preparations of cuprates and oxides with related structures are reported and the unit cells of the compounds are determined by least-squares refinements of X-ray powder diffraction data. Model calculations of the structures of $La_2Cu_{0.8}Zn_{0.2}O_4$, $La_{1.8}Ca_{0.2}CuO_4$, $LaCu_{0.5}Ni_{0.5}O_4$, $Nd_{1.85}Ce_{0.15}CuO_4$, $HoSrBaCu_3O_7$, $NdSrBaCu_3O_7$, $NdCaBaCu_3O_7$, $BaBiO_3$, $BaBi_{0.5}Cu_{0.5}O_3$, $BaBi_{0.5}La_{0.5}O_3$, were made by the profile refinement method with X-ray powder diffraction data.

Crystal growth experiments by zone melting of $Bi_2Sr_2CaCu_2O_8$ were unsuccessful as the compound decomposed. The main component in the zone melted material was $Bi_2Sr_2CuO_6$.

A partial substitution of lanthanum atoms with barium or strontium atoms in the orthorhombic compound La_2CuO_4[1] results in tetragonal $La_{2-x}Me_xCuO_4$[2] compounds (Me = Ba or Sr) with onset temperatures for superconductivity at around 30 K. The discovery of $YBa_2Cu_3O_{9-\delta}$[3] with an onset temperature for transition to superconductivity at around 90 K created a tremendous interest in the investigation of ternary and quaternary oxide systems all containing copper. The above-mentioned compounds and the quaternary oxides $Bi_2Sr_2CaCu_2O_8$[4] and $Tl_2Ba_2CaCu_2O_8$[5] with transition temperatures to superconductivity at 91 and 110 K, respectively, are members of families of layer structures with structural relations. The structure of these compounds have been determined by powder and single-crystal X-ray and neutron diffractometry, supplemented by electron diffraction, so that the structural relations between the different compounds have been established.[6]

The syntheses of these polycrystalline materials are achieved by solid state reactions in the temperature range 800–1100 °C between the components of the heterogenous mixtures made of nitrates, oxalates, carbonates and/or oxides. Crystal growth experiments have been made from the melt of mixtures of the same components as described above[7] or from salt melts,[8] but these growth experiments are hampered by the lack of information on phase diagrams of the ternary and quaternary oxide systems.

The syntheses of a selection of copper-containing compounds are described in this work. The raw materials used were in many cases heterogenous mixtures of oxides. To promote the reaction between the components the mixtures were pressed to pellets at pressures up to 400 MPa, followed by sintering at high temperatures. The methods of preparation are described in more detail below, and the obtained products are characterized by X-ray powder diffraction.

Experimental

Chemicals. The following chemicals were used in the synthesis: La_2O_3 (Aldrich Chemical Company Inc., 99.99 %), CeO_2 (Auer-Remy, 99.9 %), Nd_2O_3 (Koch-Light Laboratories Ltd., 99.9 %), Ho_2O_3 (Fluka, puriss), $CaCO_3$ (Merck, p.a.), $Sr(NO_3)_2$ (Merck, p.a.), BaO_2 (Merck, p.a.), $NiCO_3$ (Riedel de Haen, pure), CuO (Merck, p.a.), $SrCO_3$ (Merck, pure), Bi_2O_3 (Fluka, puriss), ZnO (Merck, p.a.).

CaO was made from $CaCO_3$ kept at 900 °C for 8 h. SrO was made from $SrCO_3$ kept for 3 h in a Mo crucible in a vacuum of 10^{-4} Torr at temperatures up to 1160 °C in an ADL furnace. The SrO was weighed under nitrogen in a glove box to avoid reaction with water or carbon dioxide from the atmosphere.

Preparative method. The general procedure in the preparation of a compound was as follows. Stoichiometric quantities of the starting materials were ground carefully in a B_4C mortar and pressed to pellets at a pressure of 400 MPa, in a mould made of cemented carbide. The pellets typically had a diameter of 25 mm and a thickness of up to 5 mm. The pellets were placed in boats or crucibles of Al_2O_3 in furnaces at the experimental conditions listed in Table 1. After the first sintering the pellets were reground and repressed before the second sintering. The second sintering and the following annealing were often performed in a tube furnace in a flow of 99.9 % oxygen. The experimental

Table 1. Experimental conditions for solid state reactions. Unit cell parameters in Å of reaction products.

Reaction mixtures (quantities in g)				(1) and (2) heat treatment				O_2-Flow (yes = +)	Annealing		O_2-Flow (yes = +)	Nominal composition	Ref.	Unit cell parameters		
				T/°C	Time/h	T/°C	Time/h		T/°C	Time/h				a/Å	b/Å	c/Å
-a$_2$O$_3$ 3.26	CuO 0.79			950	24	950	24	+				La_2CuO_4	1	5.426(3)	5.376(4)	13.211(7)
-a$_2$O$_3$ .78	CuO 2.15	ZnO 0.24		950	24	950	24	+				$La_2Cu_{0.9}Zn_{0.1}O_4$		5.437(2)	5.386(2)	13.167(5)
-a$_2$O$_3$ 16.3	CuO 3.18	ZnO 0.81		950	24	950	12	+				$La_2Cu_{0.8}Zn_{0.2}O_4$		5.459(3)	5.403(3)	13.143(5)
-a$_2$O$_3$ .26	CuO 0.40	NiCO$_3$ 0.59		970	24	1000	12					$La_2Cu_{0.5}Ni_{0.5}O_4$	9	3.830(1)		13.006(7)
-a$_2$O$_3$ 16.3	CuO 1.99	NiCO$_3$ 2.97		1000	24	1000	24	+				$La_2Cu_{0.5}Ni_{0.5}O_4$	9	3.843(1)		12.985(5)
.a$_2$O$_3$ .26	NiCO$_3$ 1.19			950	24	1105	20		1200	24		La_2NiO_4	10	3.881(1)		12.728(6)
.a$_2$O$_3$ .10	NiCO$_3$ 1.19	Sr(NO$_3$)$_2$ 0.21		960	44	1210	23					$La_{1.9}Sr_{0.1}NiO_4$		3.861(1)		12.732(9)
.a$_2$O$_3$ .93	NiCO$_3$ 1.19	Sr(NO$_3$)$_2$ 0.42		960	44	1210	24					$La_{1.8}Sr_{0.2}NiO_4$		3.852(1)		12.741(7)
.a$_2$O$_3$ 5.5	CuO 3.98	CaO 0.28		950	24	950	24	+	500	24	+	$La_{1.9}Ca_{0.1}CuO_4$	11	3.799(2)		13.223(6)
a$_2$O$_3$ 4.7	CuO 3.98	CaO 0.56		950	24	950	12	+	500	12	+	$La_{1.8}Ca_{0.2}CuO_4$		3.798(1)		13.237(4)
a$_2$O$_3$ 9.3	CuO 7.95	BaCuO$_2$ 3.95		980	24	1060	10					$La_{1.8}Ba_{0.2}CuO_4$	2	3.797(4)		13.349(11)
ld$_2$O$_3$ .83	CuO 0.67			960	24	1010	24					Nd_2CuO_4	12	3.962(1)		12.228(3)
ld$_2$O$_3$ .65	CuO 0.65	CeO$_2$ 0.10		970	22	1010	26					$Nd_{1.93}Ce_{0.07}CuO_4$		3.961(1)		12.219(4)
ld$_2$O$_3$ 4.9	CuO 6.36	CeO$_2$ 2.06		1020	48	1020	24		1080	48		$Nd_{1.85}Ce_{0.15}CuO_4$	13	3.968(1)		12.135(5)
aO$_2$ .39	CuO 1.59			915	23							$BaCuO_2$	14	18.377(9)		
o$_2$O$_3$ .67	CuO 7.16	BaO$_2$ 10.2		950	18	950	64	+	550	16	+	$HoBa_2Cu_3O_7$	15	3.851(2)	3.903(2)	11.730(4)
aO 1	BaO$_2$ 3.4	La$_2$O$_3$ 3.3	CuO 4.8	950	24	950	24	+	400	6	+	$LaCaBaCu_3O_7$	16	3.907(2)		11.687(4)
r(NO$_3$)$_2$ 23	BaO$_2$ 3.39	La$_2$O$_3$ 3.26	CuO 4.77	950	24	950	24	+	400	6	+	$LaSrBaCu_3O_7$		3.900(3)		11.773(12)
aO 1	BaO$_2$ 3.4	Nd$_2$O$_3$ 3.36	CuO 4.8	950	24	950	24	+	400	6	+	$NdCaBaCu_3O_7$		3.882(2)		11.663(5)
r(NO$_3$)$_2$ 23	BaO$_2$ 3.39	Nd$_2$O$_3$ 3.36	CuO 4.77	950	24	950	65	+				$NdSrBaCu_3O_7$		3.877(2)		11.675(6)
(NO$_3$)$_2$ 12	BaO$_2$ 1.7	Ho$_2$O$_3$ 1.89	CuO 2.39	950	26	1010	23					$HoSrBaCu_3O_7$		3.864(2)		11.568(7)

conditions for the preparation of $Bi_2Sr_2CaCu_2O_8$ and related compounds are listed in Table 2.

The rates of formation of $Bi_2Sr_2CaCu_2O_8$ and $Bi_2Sr_2CuO_6$ were studied in the temperature range 800–900 °C. The compositions of the reaction mixtures used are listed in Table 3. The mixtures were pressed to pellets and placed in an Al_2O_3 crucible in a crucible furnace. The reaction time was from 1 to 96 h, and the quantity of the different phases after the heat treatment was determined by X-ray diffractometry at room temperature.

Crystal growth experiments. Crystal growth of $Bi_2Sr_2CaCu_2O_8$ was investigated by zone melting in gold tubes and in tubes of Al_2O_3 in an 99.9 % oxygen atmosphere, and by floating zone melting in a 99.9 % nitrogen atmosphere using a graphite susceptor for the RF current in a HP-ADL furnace. The phases formed in the growth experiments are listed in Table 4.

Characterization. X-Ray powder patterns were recorded of all reaction products on a Stoe diffractometer with a position sensitive detector using Cu $K\alpha_1$ (λ = 1.540598 Å) radiation. The detector was curved and covered 40° in 2θ, and in each measurement of a powder pattern two positions of the detector were used, so that the pattern covered a 2θ range of 80°. The diffractometer was calibrated with a standard of silicon (a = 5.43050 Å), and with a standard of $Ag_6Ge_{10}P_{12}$ (a = 10.312 Å). Unit cell parameters of in-

Table 2. Experimental conditions for solid state reactions. Unit cell parameters in Å of reaction products.

Reaction mixtures (quantities in g)				(1) and (2) heat treatment				O_2-Flow (yes = +)	Annealing		O_2-Flow (yes = +)	Nominal composition	Ref.	Unit cell parameters		
				T/°C	Time/h	*T*/°C	Time/h		*T*/°C	Time/h				*a*/Å	*b*/Å	*c*/Å
Bi_2O_3 4.82	SrO 2.14	CaO 0.58	CuO 1.65	860	30	860	18	+	860	20	+	$Bi_2Sr_2CaCu_2O_8$	17	5.421(4)	5.455(5)	30.92(3)
Bi_2O_3 9.32	$Sr(NO_3)_2$ 8.47	CaO 1.12	CuO 3.18	825	38	850	70		860	28		$Bi_2Sr_2CaCu_2O_8$				
Bi_2O_3 4.66	$Sr(NO_3)_2$ 4.23	CuO 0.79		820	12							$Bi_2Sr_2CuO_6$	18	3.816(2)		24.73(2)
$SrBi_2O_4$ 3.42	$SrCuO_2$ 1.10			810	22							$Bi_2Sr_2CuO_6$				
$CuBi_2O_4$ 2.73	$Sr(NO_3)_2$ 2.12			820	25							$Bi_2Sr_2CuO_6$		3.798(1)		24.65(1)
Bi_2O_3 4.66	CuO 0.79			815	27							$CuBi_2O_4$	19	8.533(3)		5.836(4
Bi_2O_3 4.66	$Sr(NO_3)_2$ 2.12			815	17							$SrBi_2O_4$		Not indexed		
$Sr(NO_3)_2$ 4.23	CuO 1.59			985	26							$SrCuO_2$	20	3.573(1)	16.324(3)	3.911(1
$Sr(NO_3)_2$ 4.23	CuO 0.79			820	25							$SrCuO_2$	20	3.573(1)	16.324(3)	3.911(1
CaO 5.61	CuO 3.98			1060	65	1020	24					Ca_2CuO_3	20	12.288(6)	3.791(2)	3.266(2
Bi_2O_3 4.66	CaO 1.12	CuO 0.79		850	24							$Bi_2Ca_2CuO_6$		Not indexed		
Bi_2O_3 2.33	La_2O_3 1.63	BaO_2 3.39		800	15	825	7					$LaBa_2BiO_6$	21	4.395(2)		
Bi_2O_3 2.33	BaO_2 1.69			800	8							$BiBaO_3$	22	6.210(2) $\beta = 90.33(4)$	6.169(2)	8.696(5
Bi_2O_3 2.33	CuO 0.79	BaO_2 3.39		800	7							Ba_2CuBiO_6				
Bi_2O_3 5.14	$Sr(NO_3)_2$ 2.12			850	18	890	28		900	70		$Bi_{1-x}Sr_xO_{1.5-x/2}$ $x = 0.235$	23	3.971(1)		28.41(1)

Table 3. Experimental conditions for time resolved solid state reactions.

Reaction mixtures (quantities in g)				Temperature of heat treatment /°C	Time range /h	Nominal composition of main products
Bi_2O_3 4.66	$CaCO_3$ 1.00	$SrCO_3$ 2.95	CuO 1.58	820	1–96	$Bi_2Ca_2CuO_6$
Bi_2O_3 4.66	$Sr(NO_3)_2$ 4.23	CuO 0.79		800	1–6	$SrBi_2O_4$ and $Bi_2Sr_2CuO_6$
Bi_2O_3 4.66	$Sr(NO_3)_2$ 4.23	CuO 0.79		850	1–24	$SrBi_2O_4$ and $Bi_2Sr_2CuO_6$
Bi_2O_3 2.33	$BaCO_3$ 3.95	CuO 2.39		810	1–12	$BaBi_{0.5}Cu_{0.5}O_3$, $BaCO_3$ and CuO
Bi_2O_3 2.33	BaO_2 3.39	CuO 1.59		810	1–6	$BaBi_{0.5}Cu_{0.5}O_3$ and CuO

Table 4. Zone-melting growth experiments with $Bi_2Sr_2CaCu_2O_8$ and related compounds.

Nominal composition of sample	Crucible	Susceptor ring	Atmosphere	Pressure /MPa	Phases found in in frozen material
$Bi_2Sr_2CaCu_2O_8$	Au-tube	Au-tube	air		$Bi_2Sr_2CuO_6$
$Bi_2Sr_2CaCu_2O_8$	Al_2O_3-tube	Ir-ring	O_2	0.3	$Bi_2Sr_2CuO_6$
$Bi_2Sr_2CaCu_2O_8$	Al_2O_3-tube	Ir-ring	O_2	0.3	$Bi_2Sr_2CuO_6$
$Bi_2Sr_2Ca_2Cu_3O_{10}$		Graphite	N_2	0.5	$Bi_2Sr_2CuO_6$
$Bi_2Sr_2Ca_2Cu_3O_{10}$		Graphite	He	0.6	$Bi_2Sr_2CuO_6$
$Bi_2Sr_2CuO_6$		Graphite	N_2	0.5	$SrBi_2O_4$

dexed powder patterns were refined by a least-squares procedure,[24] or were derived in model calculation of the structure (see below). The results obtained are listed in Tables 1 and 2.

Measurements of transition to superconductivity. Measurements of possible transitions to a superconducting state of samples were made using two different methods. In the temperature range from room temperature to 77 K the magnetic susceptibility was measured with a Faraday balance. The existence of superconductivity in samples over 77 K was as well investigated qualitatively by the flux exclusion method, the Meissner effect, with a tablet of the sample cooled in liquid nitrogen and a small permanent magnet. In the temperature range 40–10 K, flux exclusion was measured on a Wheatstone bridge, containing the sample in a detector coil, and kept at cryogenic temperatures.[25] Before each measurement series the function of this apparatus was controlled using a Nb sample which showed transition to superconductivity at 9 K.

Results and discussion

The superconducting cuprates have structures with characteristic copper–oxygen layers. Two recent reviews on the structural chemistry of the superconducting cuprates by Müller-Buschbaum[26] and by Nardin *et al.*[27] have excellent drawings of the different structure types. Below are discussed the results obtained by the different preparative procedures, and model calculations are made of the structures for some of the compounds.

La_2CuO_4 and related compounds. It is possible to substitute on the lanthanum as well as on the copper sites in La_2CuO_4. Substitution of lanthanum with barium and strontium is well known from Ref. 2, and also calcium can substitute,[11] resulting in the K_2NiF_4 structure. Substitution of copper with zinc and nickel also yields the K_2NiF_4 structure, but this substitution has a negative effect on T_c that decreases.

The substitution of Cu with Zn results in an expansion in the *ab*-plane and a contraction in the direction of the *c*-axis. The orthorhombic structure of La_2CuO_4 is conserved for the solid solutions up to at least the composition $La_2Cu_{0.8}Zu_{0.2}O_4$.

The substitution of Cu with Ni also results in an expansion in the *ab*-plane and a contraction in the direction of the *c*-axis. In addition, the orthorhombic structure changes to tetragonal symmetry for $La_2Cu_{0.5}Ni_{0.5}O_4$.

For La_2NiO_4 that has the K_2NiF_4 structure[10] substitution of the lanthanum sites is possible. In a substitution with strontium the *ab*-plane shows a contraction and an expansion is observed in the direction of the *c*-axis. The tetragonal symmetry of the structure is conserved.

In contrast the substitution of copper, the substitution of lanthanum with calcium in La_2CuO_4 results in a small contraction in the *ab*-plane and an expansion in the direction of the *c*-axis, and in a tetragonal symmetry of the crystal. This was also the case for the substitution of lanthanum with barium and for the substitution of lanthanum with strontium in La_2NiO_4, see above.

In Nd_2CuO_4 substitution of Nd with Ce has been reported to result in a solid solution with transition temperature 20 K.[13] The substitution of Ce with Nd in the structure of Nd_2CuO_4 results in a contraction in the direction of the *c*-axis.

Compounds with structures related to $YBa_2Cu_3O_7$. These syntheses have all been made with BaO_2 and not with $BaCO_3$. It is an advantage to use BaO_2 in the solid state reactions in the applied temperature range because this compound is more reactive than $BaCO_3$. The two lanthanum-containing compounds $LaCaBaCu_3O_7$ and $LaSrBaCu_3O_7$ have been prepared previously.[16] The neodymium- and holmium-containing compounds $NdCaBaCu_3O_7$, $NdSrBaCu_3O_7$, and $HoSrBaCu_3O_7$ are made analogously. The T_c measurements indicate a phase transition for $NdSrBaCu_3O_7$ at 29 K.

Time-resolved experiments. The investigation of the formation of the Bi-containing cuprates is related to the crystal growth experiments with $Bi_2Sr_2CaCu_2O_8$. Melt growth experiments with $Bi_2Sr_2CaCu_2O_8$ resulted mainly in $Bi_2Sr_2CuO_6$ (see below). The time-resolved experiments were therefore performed to investigate how fast the compounds $Bi_2Sr_2CuO_6$ and $Bi_2Sr_2CaCu_2O_8$ were formed from different reaction mixtures. In addition, a number of the syntheses listed in Table 2 were made to facilitate the identification of reaction products formed in the time-resolved experiments and in the crystal growth experiments.

The melting point of Bi_2O_3 is 815 °C.[28] It is well known that the chemical reactions in a solid state reaction with a heterogenous mixture proceeds fast to an equilibrium when the temperature of reaction is close to the melting point of one of the components in the mixture. In the time resolved experiments listed in Table 3, Bi_2O_3 has the lowest melting point of the components of the mixtures, and is consumed within 1–2 h.

In the attempts to produce $Bi_2Sr_2CaCu_2O_8$ from a mixture containing the carbonates $CaCO_3$ and $SrCO_3$, the main reaction product did not contain strontium, as $SrCO_3$ is less reactive than $CaCO_3$ at 820 °C. When the mixture contained Bi_2O_3, CuO and $Sr(NO_3)_2$ in time-resolved investigations of the formation of $Bi_2Sr_2CuO_6$, the reaction products were $SrBi_2O_4$ and $Bi_2Sr_2CuO_6$.

The attempts to produce $Bi_2Sr_2CuO_6$ from mixtures made of Bi_2O_3, $Sr(NO_3)_2$ and CuO thus show that two reaction products occur in the start of the sintering experiment, $SrBi_2O_4$ and $Bi_2Sr_2CuO_6$, and $SrBi_2O_4$ is probably produced faster than $Bi_2Sr_2CuO_6$.

Attempts were made to investigate the formation of a compound with the nominal composition $BiBa_2Cu_3O_7$ that was assumed to have a $YBa_2Cu_3O_7$ structure. A fast process was observed from mixtures of Bi_2O_3, $BaCO_3$ and CuO at 810 °C. After 2 h no increase in the quantity of the reaction product was observed, but the mixture contained unreacted $BaCO_3$ and CuO. When the reaction mixture was made of Bi_2O_3, BaO_2 and CuO, the reaction was complete within 1 h at 810 °C. However, the reaction mixture still contained unreacted CuO. The powder pattern of the reaction product showed a great similarity to that of $BaBiO_3$, and it was assumed that the reaction product had the composition $BaBi_{0.5}Cu_{0.5}O_3$. A preparation according to this stoichiometry showed no excess CuO in the reaction mixture (Table 2). A compound containing lanthanum was obtained with an analogous composition, $BaBi_{0.5}La_{0.5}O_3$ (Table 2).

As expected, the solid state reactions with mixtures containing Bi_2O_3 were fast in the temperature range 800–850 °C. All the main reaction products listed in Table 3 were formed within 1 h of heat treatment, and the quantities of the reaction products did not increase much in further heat treatments.

Crystal growth experiments with $Bi_2Sr_2CaCu_2O_8$. Single crystals of $Bi_2Sr_2CaCu_2O_8$ have been grown from a KCl salt melt,[8] and single crystals have been grown in a self-flux mode[7] from a melt with the ratios of the elements Bi:Sr:Ca:Cu = 1:1:1:2. This melt is more rich in calcium and copper than the compound itself, which probably melts incongruently. This hypothesis is confirmed by the crystallization experiments made from a melt of $Bi_2Sr_2CaCu_2O_8$.

Preliminary experiments with $Bi_2Sr_2CaCu_2O_8$ showed that the compound does couple with the RF current in the ADL crystal growth furnace, but not sufficiently to produce a melt in a skull, a cold crucible, or in a floating zone growth mode, and only sintering or part melting were achieved. For this reason growth experiments were performed with crucibles as susceptors or with a ring of metal or graphite as susceptor in the zone-melting experiments as listed in Table 4. All experiments show that $Bi_2Sr_2CaCu_2O_8$ does not crystallize from a melt of that composition. The main phase in the frozen materials is $Bi_2Sr_2CuO_6$.

The recrystallization of $Bi_2Sr_2CaCu_2O_8$ from a KCl melt could be reproduced. However, if the temperature of the melt exceeded the melting point of $Bi_2Sr_2CaCu_2O_8$, decomposition also occurred.

Model calculations of structures. Profile refinement[29] has been made with the X-ray powder patterns of some of the reaction products using the program EDINP[30] and neutral atom values of the atomic scattering factors.[31] The compounds investigated and the parameters refined are listed in Table 5, and the profile fits are displayed in Fig. 1. The peak shapes of the reflections were assumed to be a convolution of Gaussian and Lorentzian functions. *U*, *V* and *W* are parameters for the Gaussian, and *T* a profile parameter for the Lorentzian shape. The observed profiles are then fitted with a calculated profile where the FWHM is given

Table 5. Parameters refined in least-squares profile refinements of X-ray powder diffraction data.

Compound	z parameters		U	V	W	T	Zero	R(%)	R_W(%)
La_2CuO_4 type structure, space group *Cmca*, Ref. 1									
$La_2Cu_{0.8}Zn_{0.2}O_4$			0.821(13)	−0.162(3)	0.080(1)	0.032(2)	0.104(1)	4.8	7.2
$La_{1.85}Ba_{0.15}CuO_4$ type structure, space group *I4/mmm*, Ref. 32									
$La_{1.80}Ca_{0.20}CuO_4$	z (La/Ca) =	0.3606(2)	0.698(13)	−0.243(5)	0.082(1)	0.109(2)	0.080(3)	3.7	7.3
La_2NiO_4 type structure, space group *I4/mmm*, Ref. 10									
$La_2Cu_{0.5}Ni_{0.5}O_4$	z (La) =	0.3607(2)	0.640(7)	−0.434(2)	0.104(6)	0.143(2)	0.000(2)	3.3	5.6
Nd_2CuO_4 type structure, space group *I4/mmm*, Ref. 12									
$Nd_{1.85}Ce_{0.15}CuO_4$	z (Nd/Ce) =	0.3556(3)	0.480(5)	−0.353(2)	0.109(1)	0.108(2)	−0.036(3)	2.8	5.2
$YBa_2Cu_3O_{6.5}$ type structure, space group *P4/mmm*, Ref. 33									
$HoSrBaCu_3O_7$	z (Sr/Ba) =	0.1919(5)	0.73(2)	−0.353(6)	0.157(1)	0.034(2)	−0.066(4)	5.3	9.1
	z (Cu2) =	0.3366(8)							
$NdSrBaCu_3O_7$	z (Sr/Ba) =	0.1756(6)	0.59(1)	−0.333(5)	0.087(1)	0.134(2)	0.060(2)	5.1	7.6
	z (Cu2) =	0.3559(10)							
$NdCaBaCu_3O_7$	z (Ca/Ba) =	0.1827(6)	0.67(1)	−0.380(4)	0.140(1)	0.132(2)	0.045(4)	3.6	5.4
	z (Cu2) =	0.3514(15)							
$BaBiO_3$ type structure, space group *I2/m*, Ref. 22									
$BaBiO_3$			1.39	−0.68	1.24	0.049	−0.11	9.2	10.5
$BaBi_{0.5}La_{0.5}O_3$			1.09	−0.52	0.133	0.049	−0.121	5.1	6.8
$BaBi_{0.5}Cu_{0.5}O_3$			1.09	−0.52	0.133	0.049	0.054	7.3	10.1

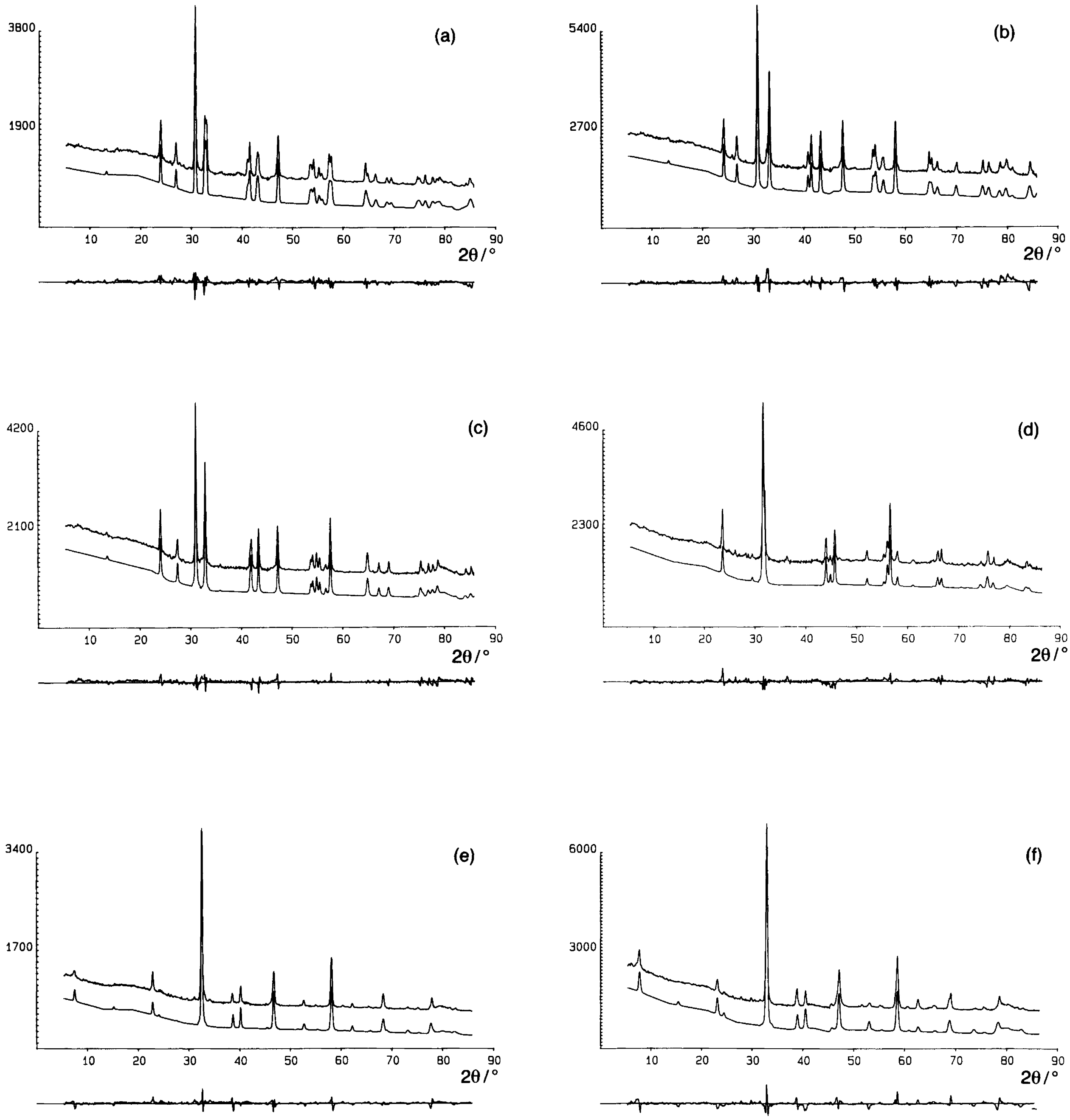

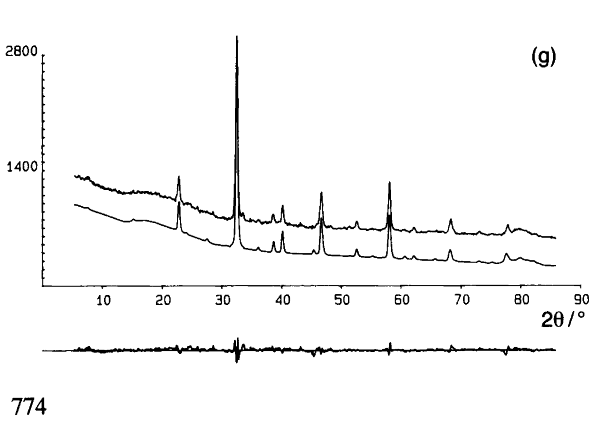

Fig. 1. X-Ray diffraction patterns used in profile refinements. Upper curves are observed and lower curves are calculated patterns. The curves below the 2θ axes are difference plots between observed and calculated patterns. (a) $La_2Cu_{0.8}Zn_{0.2}O_4$, (b) $La_{1.8}Ca_{0.2}CuO_4$, (c) $La_2Cu_{0.5}Ni_{0.5}O_4$, (d) $Nd_{1.85}Ce_{0.15}CuO_4$, (e) $NdSrBaCu_3O_7$, (f) $HoSrBaCu_3O_7$, (g) $NdCaBaCu_3O_7$.

by $(U\tan^2\theta + V\tan\theta + W)^{1/2} + T/\cos\theta$. The R values quoted are defined as follows:

$$R = \Sigma \mid y_{obs} - y_{calc} \mid / \Sigma y_{obs}$$

$$R_W = [\Sigma (y_{obs} - y_{calc})^2 W / \Sigma y^2_{obs} W]^{1/2}$$

where the y-values are the profile intensities with the background y_b subtracted and $W = 1/(y_{obs} + y_b)$. Of the positional parameters for the structures only those for the metal atoms were refined.

The model of the structure of La_2CuO_4 was used for the model calculations of $La_2Cu_{0.8}Zn_{0.2}O_4$, as this compound is orthorhombic in analogy with La_2CuO_4. The profile fit obtained is acceptable. The Zn atoms substitute in the array of the Cu atoms in the copper atom layers. The structure of $La_{1.8}Ca_{0.2}CuO_4$ was refined assuming the model of the structure of $La_{1.85}Ba_{0.15}CuO_4$, and the profile fit obtained was acceptable.

The structure of $La_2Cu_{0.5}Ni_{0.5}O_4$ was assumed to have the La_2NiO_4 structure and was refined according to that hypothesis. A statistical distribution of Cu/Ni on the *2a* site is assumed and the unit-cell volume 191.8 Å^3 is approximately equal to the average $[V(La_2CuO_4) + V(La_2NiO_4)]/2$ of 192.2 Å^3.

The structure of $Nd_{1.85}Ce_{0.15}CuO_4$ was refined using the model of the structure of Nd_2CuO_4. The unit cell of the sample investigated was significantly different from that of Nd_2CuO_4, and the profile fit obtained was acceptable. The sample did not show transition to superconductivity when cooled to 10 K, in contrast to earlier findings.[13]

The structure of $YBa_2Cu_3O_{6.5}$ was assumed for the structures of $NdCaBaCu_3O_7$, $NdSrBaCu_3O_7$ and $HoSrBaCu_3O_7$, with Ca/Ba and Sr/Ba, respectively, distributed statistically in site *2h* of space group *P4/mmm*. This gives an acceptable model in the Sr/Ba cases, and a less acceptable fit in the Ca/Ba cases, possibly indicating that the Ca atoms may also substitute on the neodymium atom sites. This problem will be further investigated by profile refinement on neutron diffraction powder data. To obtain the profile fit of $NdCaBaCu_3O_7$ displayed in Fig. 1, it was necessary to apply an occupancy for the *2h* site significantly larger than that corresponding to a statistical distribution of the calcium and barium atoms in this site.

The structure of $BaBiO_3$ has been investigated by powder neutron diffraction and profile refinements.[22] The structure is an ordered perovskite with the composition $Ba_2Bi^{3+}Bi^{5+}O_6$. The X-ray powder pattern of $BaBiO_3$ was refined using this model, and the profile fit obtained was acceptable. In substitution of bismuth with antimony the compound Ba_2SbBiO_6 is formed, and this compound has the same ordered perovskite structure.[34] Model calculations were made for the structures of $BaBi_{0.5}Cu_{0.5}O_3$ and $BaBi_{0.5}La_{0.5}O_3$ assuming an ordered perovskite structure of the Ba_2SbBiO_6 type. The profile fits were acceptable for the strong reflections, but the model could not account for some weak reflections of the two patterns. However, it is likely that the structures of $BaLa_{0.5}Bi_{0.5}O_3$ and $BaCu_{0.5}Bi_{0.5}O_3$ have great similarity with that of Ba_2SbBiO_6.

Measurements of phase transitions by the flux exclusion method. Of the samples (Table 1) investigated for superconductivity at cryogenic temperatures in the range 40–10 K, $La_{1.8}Ba_{0.2}CuO_4$, $La_2Cu_{0.5}Ni_{0.5}O_4$, Nd_2CuO_4, $Nd_{1.93}Ce_{0.07}CuO_4$, $Nd_{1.85}Ce_{0.15}CuO_4$, $NdSrBaCu_3O_7$ and $HoSrBaCu_3O_7$, only $NdSrBaCu_3O_7$ showed a transition at 29 K, that is assumed to be a transition to a superconductive state.

Conclusion

Solid state preparation of La_2CuO_4, La_2NiO_4, Nd_2CuO_4 and solid solutions of the types $La_2Cu_{1-x}Zn_xO_4$, $La_2Cu_{1-x}Ni_xO_4$, $La_{2-x}Ca_xCuO_4$, $La_{2-x}Sr_xNiO_4$ and $Nd_{2-x}Ce_xO_4$ were achieved in the temperature range 950–1020 °C. In substitution of the lanthanum atoms a contraction of the *ab*-plane of the structure takes place. Such a contraction is also observed for the compounds $La_{2-x}Ba_xCuO_4$ and $La_{2-x}Sr_xCuO_4$, and may be of importance for the superconducting properties of these compounds. In substitution of the copper sites with zinc or nickel an expansion of the *ab*-plane of the structure is observed.

A number of binary oxides were synthesized in connection with studies of the synthesis and zone melting of $Bi_2Sr_2CaCu_2O_8$. The zone-melting crystal-growth experiments with $Bi_2Sr_2CaCu_2O_8$ were not successful, as the compound decomposes by the zone-melting procedure, and the main component in the frozen material was $Bi_2Sr_2CuO_6$. The X-ray powder patterns of the binary oxides were used in comparison with the X-ray powder patterns of the zone-melted material in attempts to identify the phases present in the zone-melted materials.

The X-ray diffraction data from the Stoe diffractometer are of adequate quality for profile refinements of structural models, when the patterns have well resolved reflections. Only the metal atom positions of the structures were refined, together with unit-cell parameters and the profile parameters *U, V, W* and *T*. These are mainly instrumental parameters, but have also contributions from the compounds investigated, as particle size can be related to the width of the diffraction lines. For most of the samples investigated *U, V, W* and *T* were comparable, indicating no line-broadening from particle size effects. In the cases of $BaBiO_3$, Ba_2CuBiO_6 and Ba_2LaBiO_6 a number of reflections overlap in the diffraction lines, and it was difficult to refine *U, V, W* and *T* to values that were comparable with the values for the other profile refinements.

Acknowledgements. This investigation was supported by a grant from the Danish Natural Science Research Council concerning the study of superconducting materials. The Natural Science Research Council has also contributed financially to the crystal growth furnace and the Faraday balance used in the investigation. *Teknologistyrelsen* is acknowledged for making the Stoe X-ray powder diffractometer available to us. Mrs. M. A. Chevallier, Mrs. C. Secher, Mr. S. E. Jensen, Mr. N. J. Hansen, and Mr. M. H. Nielsen are thanked for valuable assistance.

References

1. Grande, B., Müller-Buschbaum, H. and Schweizer, M. *Z. Anorg. Allg. Chem. 428* (1977) 120.
2. Bednorz, J. G. and Müller, K. A. *Z. Phys. B64* (1986) 189.
3. Wu, M. K., Ashburn, J. R., Torng, C. J., Hor, P. H., Meng, R. L., Gao, L., Huang, Z. J., Wang, Y. Q. and Chu, C. W. *Phys. Rev. Lett. 58* (1987) 908.
4. Tallon, J. L., Buckley, R. G., Gilberd, P. W., Presland, M. R., Brown, I. W. M., Bowden, M. E., Christian, L. A. and Goguel, R. *Nature (London) 333* (1988) 153.
5. Ihara, H., Sugise, R., Hirabayashi, M., Terada, N., Jo, M., Hayashi, K., Negishi, A., Tokumoto, M., Kimura, K. and Shimomura, T. *Nature (London) 334* (1988) 510.
6. Santoro, A., Beech, F., Marezio, M. and Cava, R. J. *Physica C 156* (1988) 693.
7. You, Y. F., Li, C. Z., Wang, J. H., Chang, Y. C., Yang, Q. S., Hou, D. S., Chu, X., Mai, Z. H., Zhang, H. Y., Zheng, D. N., Ni, Y. M., Jia, S. L., Shen, D. H. and Zhao, Z. X. *Modern Phys. Lett. B2* (1988) 571.
8. Takahashi, T., Matsuyama, H., Katayama-Yoshida, H., Okabe, J., Hosoya, S., Seiki, K., Fujimoto, H., Sato, M. and Inokuchi, H. *Nature (London) 334* (1988) 691.
9. Balz, D. *Naturwissenschaften 40* (1953) 241.
10. Müller-Buschbaum, H. and Lehmann, U. *Z. Anorg. Allg. Chem. 447* (1978) 47.
11. Bednorz, J. G., Müller, K. A. and Takashige, M. *Science 236* (1987) 73.
12. Müller-Buschbaum, H. and Wollschläger, W. *Z. Anorg. Allg. Chem. 414* (1975) 76.
13. Tokura, Y., Takagi, H. and Uchida, S. *Nature (London) 337* (1989) 345.
14. Migeon, H. N., Jeannot, F., Zanne, M. and Aubry, J. *Rev. Chim. Miner. 13* (1976) 440.
15. Conroy, L. E., Christensen, A. N. and Bøttiger, J. *Acta Chem. Scand., Ser. A41* (1987) 501.
16. Fu, W. F., Zandbergen, H. W., van der Beck, C. J. and de Jongh, L. J. *Physica C 156* (1988) 133.
17. Bordet, P., Capponi, J. J., Chaillout, C., Chenavas, J., Hewat, A. W., Hewat, E. A., Hordeau, J. L., Marezio, M., Tholence, J. L. and Tranqui, D. *Physica C 153–155 (Pt. 1)* (1988) 623.
18. Torardi, C. C., Subramanian, M. A., Calabrese, J. C., Gopalakrishnan, J., McCarron, E. M., Morrissey, K. J., Askew, T. R., Flippen, R. B., Chowdhry, U. and Sleight, A. W. *Phys. Rev. B38* (1988) 225.
19. Arpe, R. and Müller-Buschbaum, H. *Z. Anorg. Allg. Chem. 426* (1976) 1.
20. Teske, C. L. and Müller-Buschbaum, H. *Z. Anorg. Allg. Chem. 379* (1970) 234.
21. Scholder, R., Ganter, K.-W., Gläser, H. and Merz, G. *Z. Anorg. Allg. Chem. 319* (1963) 375.
22. Cox, D. E. and Sleight, A. W. *Solid State Commun. 19* (1976) 969.
23. Conflant, P., Boivin, J.-C. and Thomas, D. *J. Solid State Chem. 35* (1980) 192.
24. Ersson, N. O. *Program CELLKANT,* University of Uppsala, Uppsala, Sweden. *Personal communication.*
25. Christensen, A. N., Rasmussen, S. E. and Thirup, G. *J. Solid State Chem. 34* (1980) 45.
26. Müller-Buschbaum, H. *Angew. Chem. 101* (1989) 1503.
27. Nardin, G., Randaccio, L. and Zangrando, E. *Acta Crystallogr., Sect. B45* (1989) 521.
28. Weast, R. C., Astle, M. J. and Beyer, W. H. *CRC Handbook of Chemistry and Physics,* 68th ed., CRC Press, Boca Raton, Florida 1987, p. B76.
29. Rietveld, H. M. *J. Appl. Crystallogr. 2* (1969) 65.
30. Pawley, G. S. *J. Appl. Crystallogr. 13* (1980) 630.
31. Cromer, D. T. and Mann, J. B. *Acta Crystallogr., Sect. A24* (1968) 321.
32. Jorgensen, J. D., Schuettler, H. B., Hinks, D. G., Capone, D. W., II., Zhang, K., Brodsky, M. B. and Scalapino, D. J. *Phys. Rev. Lett. 58* (1987) 1024.
33. Jorgensen, J. D., Veal, B. W., Kwok, W. K., Crabtree, G. W., Umezawa, A., Nowicki, L. J. and Panlikas, A. P. *Phys. Rev. B36* (1987) 5731.
34. Thornton, G. and Jacobson, A. J. *Acta Crystallogr., Sect. B34* (1978) 351.

Received November 22, 1989.